

# Synthesis and ‘Schizophrenic’ Micellization of Double Hydrophilic AB<sub>4</sub> Miktoarm Star and AB Diblock Copolymers: Structure and Kinetics of Micellization

Zhishen Ge,<sup>†</sup> Yuanli Cai,<sup>‡</sup> Jun Yin,<sup>†</sup> Zhiyuan Zhu,<sup>†</sup> Jingyi Rao,<sup>†</sup> and Shiyong Liu<sup>\*,†</sup>

Department of Polymer Science and Engineering, Hefei National Laboratory for Physical Sciences at the Microscale, University of Science and Technology of China, Hefei, Anhui 230026, China, and College of Chemistry, Xiangtan University, Xiangtan, Hunan 411105, China

Received September 17, 2006

Poly(*N*-isopropylacrylamide) (PNIPAM)-based tetrafunctional atom transfer radical polymerization (ATRP) macroinitiator (**1b**) was synthesized via addition reaction of mono-amino-terminated PNIPAM (**1a**) with glycidol, followed by esterification with excess 2-bromoisobutyryl bromide. Well-defined double hydrophilic miktoarm AB<sub>4</sub> star copolymer, PNIPAM-*b*-(PDEA)<sub>4</sub>, was then synthesized by polymerizing 2-(diethylamino)ethyl methacrylate (DEA) via ATRP in 2-propanol at 45 °C using **1b**, where PDEA was poly(2-(diethylamino)ethyl methacrylate). For comparison, PNIPAM-*b*-PDEA linear diblock copolymer with comparable molecular weight and composition to that of PNIPAM-*b*-(PDEA)<sub>4</sub> was prepared via reversible addition–fragmentation chain transfer (RAFT) polymerization. The pH- and thermoresponsive ‘schizophrenic’ micellization behavior of the obtained PNIPAM<sub>65</sub>-*b*-(PDEA<sub>63</sub>)<sub>4</sub> miktoarm star and PNIPAM<sub>70</sub>-*b*-PDEA<sub>260</sub> linear diblock copolymers were investigated by <sup>1</sup>H NMR and laser light scattering (LLS). In acidic solution and elevated temperatures, PNIPAM-core micelles were formed; whereas at slightly alkaline conditions and room temperature, structurally inverted PDEA-core micelles were formed. The size of the PDEA-core micelles of PNIPAM<sub>65</sub>-*b*-(PDEA<sub>63</sub>)<sub>4</sub> is much smaller than that of PNIPAM<sub>70</sub>-*b*-PDEA<sub>260</sub>. Furthermore, the pH-induced micellization kinetics of the AB<sub>4</sub> miktoarm star and AB block copolymers were investigated by the stopped-flow light scattering technique upon a pH jump from 4 to 10. Typical kinetic traces for the micellization of both types of copolymers can be well fitted with double-exponential functions, yielding a fast ( $\tau_1$ ) and a slow ( $\tau_2$ ) relaxation processes.  $\tau_1$  for both copolymers decreased with increasing polymer concentration.  $\tau_2$  was independent of polymer concentration for PNIPAM<sub>65</sub>-*b*-(PDEA<sub>63</sub>)<sub>4</sub>, whereas it decreased with increasing polymer concentration for PNIPAM<sub>70</sub>-*b*-PDEA<sub>260</sub>. The chain architectural effects on the micellization properties and the underlying mechanisms were discussed in detail.

## Introduction

Stimuli-responsive double hydrophilic block copolymers (DHBCs) represent a new class of amphiphilic block copolymers,<sup>1–3</sup> which can self-assemble into one or more types of micellar aggregates in water if external conditions such as temperature, pH, and ionic strength are finely adjusted.<sup>1–19</sup> DHBCs have

received a great deal of attention in the past few years due to their potential applications in pharmaceuticals, coatings, rheology modifiers, colloidal stabilization, and templates for the preparation of nanomaterials.<sup>1</sup> Past studies of DHBCs mainly deal with linear AB diblock copolymers.<sup>1–18</sup> The critical micellization concentration (cmc), aggregation number ( $N_{agg}$ ), shape, and size of the micelles are determined by the solution conditions, the relative block lengths, and the molecular weights of DHBCs.<sup>1,2,20</sup>

Theoretically, the chain architectures of block copolymers will also play a critical role in determining the micellization properties.<sup>21,22</sup> Experimentally,<sup>23–37</sup> it has been known to us that

\* To whom correspondence should be addressed. Email: sliu@ustc.edu.cn.

<sup>†</sup> University of Science and Technology of China.

<sup>‡</sup> Xiangtan University.

(1) Colfen, H. *Macromol. Rapid Commun.* **2001**, *22*, 219–252.

(2) Gohy, J. F. *Adv. Polym. Sci.* **2005**, *190*, 65–136.

(3) Riess, G. *Prog. Polym. Sci.* **2003**, *28*, 1107–1170.

(4) Butun, V.; Billingham, N. C.; Armes, S. P. *J. Am. Chem. Soc.* **1998**, *120*, 11818–11819.

(5) Rodriguez-Hernandez, J.; Lecommandoux, S. *J. Am. Chem. Soc.* **2005**, *127*, 2026–2027.

(6) Maeda, Y.; Mochiduki, H.; Ikeda, I. *Macromol. Rapid Commun.* **2004**, *25*, 1330–1334.

(7) Arotcarena, M.; Heise, B.; Ishaya, S.; Laschewsky, A. *J. Am. Chem. Soc.* **2002**, *124*, 3787–3793.

(8) Virtanen, J.; Arotcarena, M.; Heise, B.; Ishaya, S.; Laschewsky, A.; Tenhu, H. *Langmuir* **2002**, *18*, 5360–5365.

(9) Andre, X.; Zhang, M. F.; Muller, A. H. E. *Macromol. Rapid Commun.* **2005**, *26*, 558–563.

(10) Schilli, C. M.; Zhang, M. F.; Rizzardo, E.; Thang, S. H.; Chong, Y. K.; Edwards, K.; Karlsson, G.; Muller, A. H. E. *Macromolecules* **2004**, *37*, 7861–7866.

(11) Gil, E. S.; Hudson, S. A. *Prog. Polym. Sci.* **2004**, *29*, 1173–1222.

(12) Alarcon, C. D. H.; Pennadam, S.; Alexander, C. *Chem. Soc. Rev.* **2005**, *34*, 276–285.

(13) Dai, S.; Ravi, P.; Tam, K. C.; Mao, B. W.; Gang, L. H. *Langmuir* **2003**, *19*, 5175–5177.

(14) Gan, L. H.; Ravi, P.; Mao, B. W.; Tam, K. C. *J. Polym. Sci., Part A: Polym. Chem.* **2003**, *41*, 2688–2695.

(15) Butun, V.; Liu, S.; Weaver, J. V. M.; Bories-Azeau, X.; Cai, Y.; Armes, S. P. *React. Funct. Polym.* **2006**, *66*, 157–165.

(16) Liu, S. Y.; Armes, S. P. *Angew. Chem., Int. Ed.* **2002**, *41*, 1413–1416.

(17) Liu, S. Y.; Armes, S. P. *Langmuir* **2003**, *19*, 4432–4438.

(18) Sumerlin, B. S.; Lowe, A. B.; Thomas, D. B.; Convertine, A. J.; Donovan, M. S.; McCormick, C. L. *J. Polym. Sci., Part A: Polym. Chem.* **2004**, *42*, 1724–1734.

(19) Poe, G. D.; McCormick, C. L. *J. Polym. Sci., Part A: Polym. Chem.* **2004**, *42*, 2520–2533.

(20) Hamley, I. W. *The Physics of Block Copolymers*; Oxford University Press: Oxford, 1998.

(21) Jabbarzadeh, A.; Atkinson, J. D.; Tanner, R. I. *Macromolecules* **2003**, *36*, 5020–5031.

(22) Tezuka, Y.; Oike, H. *J. Am. Chem. Soc.* **2001**, *123*, 11570–11576.

(23) Tezuka, Y.; Ohashi, F. *Macromol. Rapid Commun.* **2005**, *26*, 608–612.

(24) Cai, Y. L.; Tang, Y. Q.; Armes, S. P. *Macromolecules* **2004**, *37*, 9728–9737.

(25) Cai, Y. L.; Armes, S. P. *Macromolecules* **2005**, *38*, 271–279.

(26) Hou, S. J.; Chaikov, E. L.; Taton, D.; Gnanou, Y. *Macromolecules* **2003**, *36*, 3874–3881.

(27) Mountrichas, G.; Mpiri, M.; Pispas, S. *Macromolecules* **2005**, *38*, 940–947.

(28) Pispas, S.; Hadjichristidis, N.; Potemkin, I.; Khokhlov, A. *Macromolecules* **2000**, *33*, 1741–1746.

(29) Hadjichristidis, N.; Iatrou, H.; Pitsikalis, M.; Pispas, S.; Avgeropoulos, A. *Prog. Polym. Sci.* **2005**, *30*, 725–782.

nonlinear block copolymers typically exhibit intriguing and unique characteristics during micellization and/or microphase separation in the condensed state. Hadjichristidis et al.<sup>32</sup> synthesized nonlinear super-H-shaped block copolymers of the PI<sub>3</sub>PSPI<sub>3</sub> type, where PI was protonated polyisoprene and PS was polystyrene. The micellization behavior of these block copolymers with different PS contents was investigated in *n*-decane, which is a selective solvent for the PI arms. It was found that super-H block copolymers with a large fraction ( $\geq 33$  mol %) of PS can self-assemble into quite monodisperse and spherical micelles, while those with a small PS content ( $\leq 14$  mol %) form unimolecular micelles (nonaggregated). Just recently, we have synthesized H-shaped (PDEA)<sub>2</sub>PPO(PDEA)<sub>2</sub> and (PDEA)<sub>4</sub>PPO(PDEA)<sub>4</sub> star-*b*-linear-*b*-star block copolymers, where PPO was poly(propylene oxide) and PDEA was poly(2-(diethylamino)ethyl methacrylate).<sup>38</sup> At pH 8.5 and 5 °C, (PDEA)<sub>2</sub>PPO<sub>33</sub>(PDEA)<sub>2</sub> and (PDEA)<sub>4</sub>PPO<sub>33</sub>(PDEA)<sub>4</sub> star-*b*-linear-*b*-star block copolymers formed much larger PDEA-core micelles compared to PPO-*b*-PDEA with comparable PPO content and molecular weight. The formed PDEA-core micelles took a "flower-like" structure in which soluble PPO central block formed loops surrounding the insoluble PDEA core. In marked contrast to PPO-*b*-PDEA, upon heating the aqueous solutions at pH 6.4, both types of nonlinear block copolymers formed unimolecular micelles with the core consisting of a single PPO block.<sup>38</sup>

In the category of nonlinear block copolymers, asymmetric AB<sub>2</sub> miktoarm (Y-shaped) star copolymers have been extensively studied. Pispas et al.<sup>28</sup> studied the micellization properties of PS-*b*-(PI)<sub>2</sub>, (PS)<sub>2</sub>-*b*-PI, and PS-*b*-PI copolymers. In a selective solvent for the PI block, the aggregation number and size of the PS-core micelles increase in the order PS-*b*-(PI)<sub>2</sub> < (PS)<sub>2</sub>-*b*-PI < PS-*b*-PI. They have also developed a simple scaling theory considering the free energy contributions from the core, the corona, and the interfacial region of the micelles of block copolymers with different architectures. Armes et al.<sup>24,25</sup> recently reported the preparation of stimulus-responsive Y-shaped (AB)<sub>2</sub> DHBCs, which can self-assemble into micelles with different dimensions compared to those formed by the linear diblock copolymers.

We have been interested with the micellization kinetics of DHBCs in the past 2 years. Linear and nonlinear block copolymers should differ considerably in both their micellar structures and the unimer-to-micelle transition kinetics.<sup>39–42</sup> Quite recently, Pispas et al.<sup>27</sup> reported the first study of the micellization kinetics of nonlinear block copolymers. They synthesized a (PSPI)<sub>8</sub> star block copolymer with PI being the inner blocks. In ethyl acetate, a selective solvent for the PS outer star blocks, (PSPI)<sub>8</sub> form

multimolecular micelles with the core consisting of PI inner blocks upon cooling from 60 to 30 °C. The temperature-induced micellization process took  $\sim 250$  s, which was shorter than that of the linear diblock copolymer. In this case, the temperature jump was realized by transferring the cell containing the unimer solution preheated at 60 °C to the light-scattering apparatus thermostated at 30 °C. This partially limited the accuracy of kinetics for the early stages because of the long thermal equilibrium period needed.<sup>43</sup> We recently found that stopped-flow light scattering provides a quite convenient technique to obtain the stimuli-responsive micellization kinetics, the dead time of which can be down to a few milliseconds.<sup>44–46</sup> We have studied the pH-induced micellization kinetics of poly(glycerol monomethacrylate)-*b*-poly(2-(dimethylamino)ethyl methacrylate)-*b*-poly(2-(diethylamino)ethyl methacrylate) (PGMA-*b*-PDMA-*b*-PDEA),<sup>45</sup> and the micelle inversion kinetics of poly(4-vinylbenzoic acid)-*b*-poly(*N*-(morpholino)ethyl methacrylate) (PVBA-*b*-PMEMA) employing the stopped-flow technique.<sup>46</sup>

It is well-known that poly(*N*-isopropylacrylamide) (PNIPAM) homopolymer dissolves in cold, dilute aqueous solution but becomes insoluble at  $\sim 32$  °C.<sup>47</sup> While poly(2-(diethylamino)ethyl methacrylate) (PDEA) homopolymer is soluble in acidic solution as a weak cationic polyelectrolyte (due to protonation of the tertiary amine residues) but precipitates out of solution at around neutral pH.<sup>48,49</sup> Herein, we synthesized a double hydrophilic AB<sub>4</sub> miktoarm star copolymer of *N*-isopropylacrylamide (NIPAM) and 2-(diethylamino)ethyl methacrylate (DEA), PNIPAM-*b*-(PDEA)<sub>4</sub>, and linear PNIPAM-*b*-PDEA diblock copolymer with comparable composition and molecular weight, employing atom transfer radical polymerization (ATRP) and reversible addition-fragmentation chain transfer (RAFT) techniques, respectively. In acidic solution and elevated temperatures, both copolymers should form PNIPAM-core micelles; while in slight alkaline solution and room temperature, PDEA-core micelles should form. The stimuli-responsive 'schizophrenic' micellization behavior was studied by a combination of <sup>1</sup>H NMR and laser light scattering (LLS). Most importantly, the pH-induced kinetics of the formation of PDEA-core micelles of PNIPAM-*b*-(PDEA)<sub>4</sub> and PNIPAM-*b*-PDEA was studied for the first time using stopped-flow pH jump. The chain architectural effects on the micellization properties and the underlying mechanisms were discussed in detail by comparing the kinetics and mechanism of pH-induced micellization of the nonlinear AB<sub>4</sub> star copolymer and linear AB diblock copolymer.

## Experimental Section

**Materials.** *N*-Isopropylacrylamide (NIPAM, 97%, Tokyo Kasei Kogyo Co.) was purified by recrystallization from a mixture of benzene and *n*-hexane (2/3, v/v). 2,2'-Azobis(isobutyronitrile) (AIBN) was recrystallized from ethanol. 2-(Diethylamino)ethyl methacrylate (DEA, Aldrich) was passed through basic alumina columns, vacuum distilled from CaH<sub>2</sub>, and stored at  $-20$  °C prior to use. 2-Cyanoprop-2-yl dithiobenzoate (CPDB) was synthesized

(30) Hadjichristidis, N.; Pitsikalis, M.; Iatrou, H. *Adv. Polym. Sci.* **2005**, *189*, 1–124.

(31) Hadjichristidis, N.; Pitsikalis, M.; Pispas, S.; Iatrou, H. *Chem. Rev.* **2001**, *101*, 3747–3792.

(32) Iatrou, H.; Willner, L.; Hadjichristidis, N.; Halperin, A.; Richter, D. *Macromolecules* **1996**, *29*, 581–591.

(33) Lambeth, R. H.; Ramakrishnan, S.; Mueller, R.; Poziemski, J. P.; Miguel, G. S.; Markoski, L. J.; Zukoski, C. F.; Moore, J. S. *Langmuir* **2006**, *22*, 6352–6360.

(34) Hadjichristidis, N.; Pispas, S. *Adv. Polym. Sci.* **2006**, *200*, 37–55.

(35) Pispas, S.; Hadjichristidis, N.; Mays, J. W. *Macromolecules* **1996**, *29*, 7378–7385.

(36) Pitsikalis, M.; Woodward, J.; Mays, J. W.; Hadjichristidis, N. *Macromolecules* **1997**, *30*, 5384–5389.

(37) Pitsikalis, M.; Sioula, S.; Pispas, S.; Hadjichristidis, N.; Cook, D. C.; Li, J. B.; Mays, J. W. *J. Polym. Sci., Part A: Polym. Chem.* **1999**, *37*, 4337–4350.

(38) Xu, J.; Ge, Z. S.; Zhu, Z. Y.; Luo, S. Z.; Liu, H.; Liu, S. Y. *Macromolecules* **2006**, *39*, 8178–8185.

(39) Dormidontova, E. E. *Macromolecules* **1999**, *32*, 7630–7644.

(40) Halperin, A.; Alexander, S. *Macromolecules* **1989**, *22*, 2403–2412.

(41) Honda, C.; Abe, Y.; Nose, T. *Macromolecules* **1996**, *29*, 6778–6785.

(42) Honda, C.; Hasegawa, Y.; Hirunuma, R.; Nose, T. *Macromolecules* **1994**, *27*, 7660–7668.

(43) Chu, B.; Ying, Q. C.; Grosberg, A. Y. *Macromolecules* **1995**, *28*, 180–189.

(44) Jiang, X. Z.; Luo, S. Z.; Armes, S. P.; Shi, W. F.; Liu, S. Y. *Macromolecules* **2006**, *39*, 5987–5994.

(45) Zhu, Z. Y.; Armes, S. P.; Liu, S. Y. *Macromolecules* **2005**, *38*, 9803–9812.

(46) Wang, D.; Yin, J.; Zhu, Z.; Ge, Z.; Liu, H.; Armes, S. P.; Liu, S. *Macromolecules* **2006**, *39*, 7378–7385.

(47) Schild, H. G. *Prog. Polym. Sci.* **1992**, *17*, 163–249.

(48) Liu, S. Y.; Weaver, J. V. M.; Tang, Y. Q.; Billingham, N. C.; Armes, S. P.; Tribe, K. *Macromolecules* **2002**, *35*, 6121–6131.

(49) Liu, S. Y.; Billingham, N. C.; Armes, S. P. *Angew. Chem., Int. Ed.* **2001**, *40*, 2328–2331.

according to literature method.<sup>50</sup> Tris(2-(dimethylamino)ethyl)amine (Me<sub>6</sub>TREN) was prepared as described in the literature.<sup>51</sup> Glycidol (96%) was purchased from Aldrich and distilled just prior to use. Copper(I) bromide (CuBr), 2,2'-bipyridine (bpy), 2-bromoisobutryl bromide, 2-aminoethanethiol hydrochloride (AET·HCl), and triethylamine were purchased from Aldrich and used without further purification. Other reagents were purchased from Shanghai Experiment Reagent Co., Ltd. Mono-amino-terminated PNIPAM was synthesized by the free radical polymerization of NIPAM in methanol at 60 °C using AIBN and AET·HCl as initiator and chain transfer reagent, respectively.<sup>52–54</sup> The crude polydisperse amino-terminated PNIPAM (**1a**) was dissolved in water and further purified by successive dialysis using semipermeable membranes with cutoff molar masses of 7000 and 14 000 g/mol, respectively. Amino-terminated PNIPAM fraction with molar mass within this range was collected and freeze-dried. The purified **1a** has a number-average molecular weight,  $M_n$ , of 7400 (the degree of polymerization, DP = 65) and a polydispersity,  $M_w/M_n$ , of 1.31, as determined by GPC analysis.

**Sample Preparation.** *Synthesis of PNIPAM-Based Tetrafunctional ATRP Macroinitiator (1b).* A solution of **1a** (3.33 g, 0.45 mmol) in 5 mL THF was added dropwise into the solution of glycidol (0.12 mL, 1.8 mmol) in 10 mL THF over a period of 0.5 h under nitrogen protection at 0 °C.<sup>55–57</sup> The reaction mixture was then stirred for 2 h at room temperature. The mixture was precipitated into anhydrous diethyl ether twice. The product, PNIPAM-(OH)<sub>4</sub>, was collected by filtration and then dried in a vacuum oven overnight at room temperature.

PNIPAM-(OH)<sub>4</sub> (3.0 g, 0.4 mmol) was added, along with triethylamine (0.56 mL, 4.0 mmol) and anhydrous THF (50 mL), to a dried 100 mL one-necked round-bottomed flask immersed in an ice bath.<sup>24,25,38</sup> This solution was stirred for 30 min, and 2-bromoisobutryl bromide (0.49 mL, 4.0 mmol) was then added dropwise to the flask via syringe over 1 h. The reaction mixture was stirred at 20 °C for a further 48 h. The resulting insoluble triethylamine hydrobromide salt was removed by filtration, and most of the THF was removed by rotary evaporation prior to precipitation into anhydrous diethyl ether for four times. The product, PNIPAM-Br<sub>4</sub> (**1b**) was collected by filtration and then dried in a vacuum oven at room temperature.

*ATRP Protocol for the Synthesis of Miktoarm AB<sub>4</sub> Star Copolymer.* The PNIPAM-based ATRP macroinitiator (**1b**), 1.63 g, 0.2 mmol, 0.8 mmol initiating sites), DEA (11.2 mL, 56 mmol), Me<sub>6</sub>TREN (0.184 g, 0.8 mmol), and 2-propanol (11.2 mL) were added to the reaction flask, and the solution was degassed by two freeze–thaw cycles. After the solution temperature was increased to 45 °C, CuCl (79.6 mg, 0.8 mmol) was introduced as a solid into the reaction flask to start the polymerization at this temperature. The reaction solution became dark green and more viscous as polymerization proceeded. After about 12 h, the conversion was higher than 95%. The reaction mixture was diluted with THF and passed through a neutral Al<sub>2</sub>O<sub>3</sub> column to remove the residual ATRP catalyst. After the solvent was removed, the product was extracted with ice-cold water (0 °C, pH 9) several times to remove any traces of unfunctionalized PNIPAM and then dissolved in acidic water (pH 4). The aqueous solution was dialyzed by using semipermeable membrane (cutoff molar mass, 14000 Da) for 1 day to further remove any residual DEA monomer and PNIPAM. PNIPAM-*b*-(PDEA)<sub>4</sub> was recovered by freeze-drying. GPC analysis revealed an  $M_n$  of 54400 and an  $M_w/M_n$  of 1.23.

*RAFT Protocol for the Synthesis of PNIPAM-*b*-PDEA Diblock Copolymer.* PNIPAM (6.78 g, 0.06 mol), CPDB (0.1326 g, 0.6 mmol), and AIBN (19.7 mg, 0.12 mmol) were dissolved in dioxane. The [monomer]/[CPDB]/[AIBN] ratio was 100/1/0.2. The solution was degassed by two freeze–thaw cycles before the reaction was left for 24 h at 80 °C in an oil bath. Before the reaction was quenched into liquid N<sub>2</sub>, samples were collected and analyzed by <sup>1</sup>H NMR to assess the conversion. The quenched reaction mixture was diluted with dichloromethane before being precipitated in cold diethyl ether to remove all unreacted monomer. The product was dried in vacuo at room temperature for 24 h. GPC analysis revealed an  $M_n$  of 7900 and an  $M_w/M_n$  of 1.09.

The resulting PNIPAM homopolymer (**2a**, 0.395 g, 0.05 mmol) was employed as a macroRAFT agent for the polymerization of DEA (3.01 mL, 15 mmol). The polymerization was conducted in 1,4-dioxane (4 mL) at 80 °C with AIBN (1.6 mg, 0.01 mmol) as the initiator. The [monomer]/[**2a**]/[initiator] ratio was 300/1/0.2. The solution was degassed by two freeze–thaw cycles before the reaction mixture was stirring at 80 °C in an oil bath. Before the reaction was quenched, samples were collected and analyzed by <sup>1</sup>H NMR to assess the conversion. After about 24 h, the reaction mixture was diluted with dichloromethane. After solvent evaporation, the products were extracted with ice-cold water (0 °C, pH 9) several times to remove any traces of unreacted PNIPAM macroinitiator and then dissolved in acidic water (pH 4). The aqueous solution was then dialyzed by using semipermeable membrane (cutoff molar mass, 14000 Da) for 1 day to remove residual DEA monomer and unfunctionalized PNIPAM. The copolymer solution was recovered by freeze drying. GPC analysis revealed an  $M_n$  of 55200 g/mol and a polydispersity of 1.32.

**Characterization.** *Nuclear Magnetic Resonance (NMR) Spectroscopy.* All <sup>1</sup>H NMR spectra were recorded on a Bruker 300 MHz spectrometer using CDCl<sub>3</sub> or D<sub>2</sub>O as solvents.

*Gel Permeation Chromatography (GPC).* Molecular weight distributions were determined by GPC using a series of two linear Styragel columns HT3, HT4 and a column temperature of 35 °C. A Waters 1515 pump and Waters 2414 differential refractive index detector (set at 30 °C) were used. The eluent was THF at a flow rate of 1.0 mL/min. A series of six low polydispersity polystyrene standards with molecular weights ranging from 800 to 400000 g/mol were used for the GPC calibration.

*Laser Light Scattering (LLS).* A commercial spectrometer (ALV/DLS/SLS-5022F) equipped with a multi-tau digital time correlator (ALV5000) and a cylindrical 22 mW Uniphase He–Ne laser ( $\lambda_0 = 632$  nm) as the light source was used. In static LLS (SLS), we can obtain the weight-average molar mass ( $M_w$ ) and the *z*-average root-mean square radius of gyration ( $\langle R_g^2 \rangle^{1/2}$  or written as  $\langle R_g \rangle$ ) of polymer chains in a dilute solution from the angular dependence of the excess absolute scattering intensity, known as Rayleigh ratio  $R_{vv}(q)$ , as

$$\frac{KC}{R_{vv}(q)} \approx \frac{1}{M_w} \left( 1 + \frac{1}{3} \langle R_g^2 \rangle q^2 \right) + 2A_2C \quad (1)$$

where  $K = 4\pi^2 n^2 (dn/dc)^2 / (N_A \lambda_0^4)$  and  $q = (4\pi n / \lambda_0) \sin(\theta/2)$  with  $N_A$ ,  $dn/dc$ ,  $n$ , and  $\lambda_0$  being the Avogadro number, the specific refractive index increment, the solvent refractive index, and the wavelength of the laser light in a vacuum, respectively; and  $A_2$  is the second virial coefficient.  $dn/dc$  was determined using an Optokem differential refractometer operating at 632.8 nm. Strictly speaking, here  $R_{vv}(q)$  should be  $R_{vu}(q)$  because there is no analyzer before the detector. However, the depolarized scattering of the solution studied is insignificant so that  $R_{vu}(q) \sim R_{vv}(q)$ . Also note that in this study, the sample solution was so dilute that the extrapolation of  $C \rightarrow 0$  was not necessary, and the term  $2A_2C$  in eq 1 can be neglected.

In dynamic LLS (DLS), the Laplace inversion of each measured intensity, intensity–time correlation function  $G^{(2)}(q, t)$  in the self-beating mode, can lead to a line-width distribution  $G(\Gamma)$ . For a pure diffusive relaxation,  $\Gamma$  is related to the translational diffusion coefficient  $D$  by  $(\Gamma/q^2)_{C \rightarrow 0, q \rightarrow 0} \rightarrow D$ , or further to the hydrodynamic radius  $R_h$  via the Stokes–Einstein equation,  $R_h = (k_B T / 6\pi\eta_0) / D$ ,

(50) Moad, G.; Chiefari, J.; Chong, Y. K.; Krstina, J.; Mayadunne, R. T. A.; Postma, A.; Rizzardo, E.; Thang, S. H. *Polym. Int.* **2000**, *49*, 993–1001.

(51) Queffelec, J.; Gaynor, S. G.; Matyjaszewski, K. *Macromolecules* **2000**, *33*, 8629.

(52) Chen, G. H.; Hoffman, A. S. *Nature* **1995**, *373*, 49–52.

(53) Zhang, J. X.; Qiu, L. Y.; Zhu, K. J.; Yin, Y. *Macromol. Rapid Commun.* **2004**, *25*, 1563–1567.

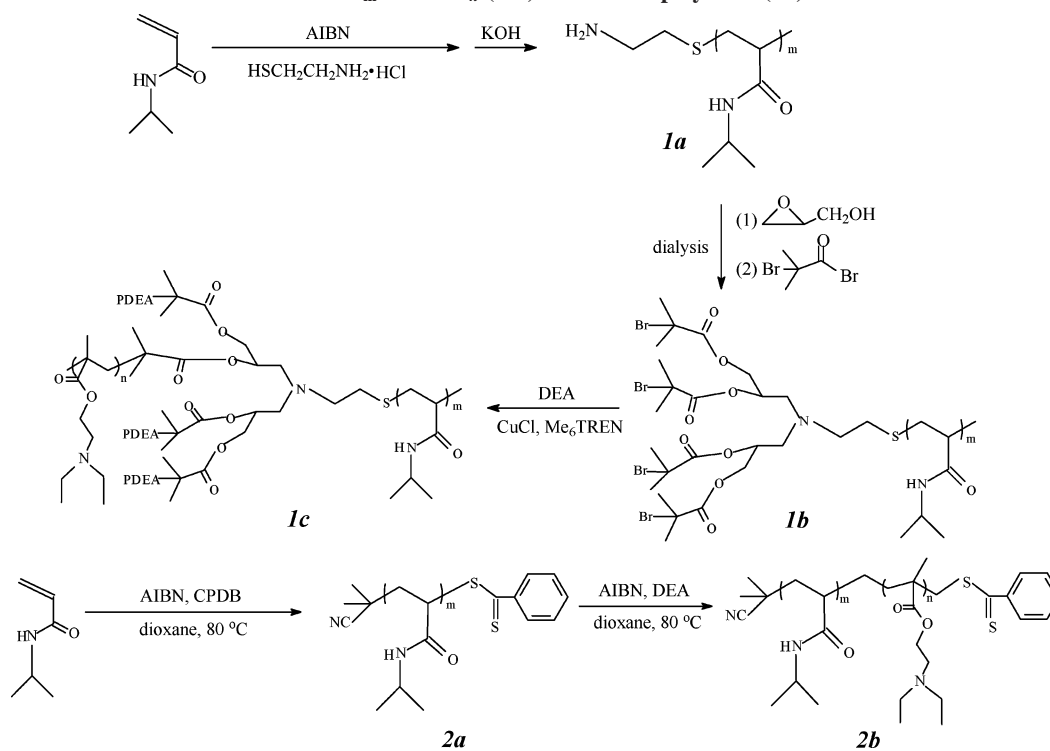
(54) Durand, A.; Hourdet, D. *Polymer* **1999**, *40*, 4941–4951.

(55) Mori, H.; Lanzendorfer, M. G.; Muller, A. H. E.; Klee, J. E. *Macromolecules* **2004**, *37*, 5228–5238.

(56) Mori, H.; Lanzendorfer, M. G.; Muller, A. H. E.; Klee, J. E. *Langmuir* **2004**, *20*, 1934–1944.

(57) Mori, H.; Muller, A. H. E.; Klee, J. E. *J. Am. Chem. Soc.* **2003**, *125*, 3712–3713.

**Scheme 1. Schematic Illustration for the Preparation of PNIPAM<sub>m</sub>-b-(PDEA<sub>n</sub>)<sub>4</sub> (AB<sub>4</sub>) Miktoarm Star (1c) and PNIPAM<sub>m</sub>-b-PDEA<sub>n</sub> (AB) Diblock Copolymers (2b)**



where  $k_B$ ,  $T$ , and  $\eta_0$  are the Boltzmann constant, the absolute temperature, and the solvent viscosity, respectively.

**Transmittance Measurements.** The transmittance of the aqueous solution was acquired on a Unico UV/vis 2802PCS spectrophotometer and measured at a wavelength of 600 nm using a thermostatically controlled cuvette.

**Stopped-Flow with Light-Scattering Detection.** Stopped-flow studies were carried out using a Bio-Logic SFM300/S stopped-flow instrument. The SFM-3/S contains three stepmotor-driven 10 mL syringes (S1, S2, S3) that can be operated independently to carry out single- or double-mixing. The SFM-300/S stopped-flow apparatus is attached to a MOS-250 spectrometer; kinetic data were fitted using a Biokine program supplied by Bio-Logic. For light-scattering detection at a fixed scattering angle of  $90^\circ$ , both the excitation and emission wavelengths were adjusted to 335 nm with 10 nm slits. The dynamic trace at each composition is averaged from 10 successive shots. Using FC-08 or FC-15 flow cells, the typical dead times were 1.1 and 2.6 ms, respectively. The solution temperature was maintained at  $20^\circ\text{C}$  by circulating water around the syringe chamber and the observation head. All solutions prior to loading into the motor-driven syringes were clarified by  $0.45\ \mu\text{m}$  Millipore nylon filters.

## Results and Discussion

The syntheses of miktoarm star copolymers have been extensively explored. Various techniques such as high vacuum anionic polymerization,<sup>27–31,34,58–60</sup> ATRP,<sup>24,25,61</sup> RAFT,<sup>30</sup> ring-opening polymerization (ROP),<sup>62</sup> nitroxide-mediated radical polymerization (NMP), or a combination of them<sup>63–69</sup> have been

developed. The general synthetic routes used for the preparation of PNIPAM-*b*-(PDEA)<sub>4</sub> miktoarm star copolymers and linear PNIPAM-*b*-PDEA diblock copolymers are shown in Scheme 1. The first step involved in the preparation of tetrafunctional PNIPAM-based ATRP macroinitiator, **1b**, is the addition reaction between the terminal primary amine group of **1a** with glycidol, forming the tetrahydroxyl-terminated PNIPAM, PNIPAM-(OH)<sub>4</sub>. This is followed by the esterification of terminal hydroxyl groups with excess 2-bromoisobutyryl bromide, resulting in the ATRP macroinitiators **1b**. PNIPAM-*b*-(PDEA)<sub>4</sub> is obtained by polymerizing DEA via ATRP using **1b** as macroinitiator.<sup>24,25,38</sup>

**Synthesis of Miktoarm AB<sub>4</sub> Star Copolymer Using the PNIPAM-Based ATRP Macroinitiator (1b).** A mono-amino-terminated homopolymer, **1a**, was used as a precursor for the synthesis of tetrafunctional ATRP macroinitiator. The terminal primary amine group of **1a** was reacted with excess glycidol ( $[\text{glycidol}]/[\text{NH}_2] = 4.0$ ), affording a tetrahydroxyl-terminated PNIPAM.<sup>55–57</sup> The addition reaction between terminal primary amine group and glycidol is evidenced by the appearance of new signals at  $\delta = 3.4\text{--}3.7$  ppm ( $f + g$ ), which were ascribed to the methylene protons next to the four terminal hydroxyl groups (Figure 1a and 1b). In Figure 1b, the ratio of integrals of peak *b* to  $f + g$  is  $\sim 10/1$ , this lead us to conclude that that the starting material, PNIPAM-NH<sub>2</sub> (**1a**), was quantitatively transformed into tetrahydroxyl-terminated PNIPAM.

The tetrafunctional ATRP macroinitiator, **1b**, was obtained by esterification of this tetrahydroxyl-terminated PNIPAM with excess 2-bromoisobutyryl bromide. A new signal at  $\delta = 4.2\text{--}4.4$  ppm appears, which was ascribed to the ester methylene

(58) Mavroudis, A.; Avgeropoulos, A.; Hadjichristidis, N.; Thomas, E. L.; Lohse, D. J. *Chem. Mater.* **2006**, *18*, 2164–2168.

(59) Velis, G.; Hadjichristidis, N. *Macromolecules* **1999**, *32*, 534–536.

(60) Wang, X.; Xia, J.; He, J.; Yu, F.; Li, A.; Xu, J.; Lu, H.; Yang, Y. *Macromolecules* **2006**, *39*, 6898–6904.

(61) Chen, J. F.; Wang, X. Z.; Liao, X. J.; Zhang, H. L.; Wang, X. Y.; Zhou, Q. F. *Macromol. Rapid Commun.* **2006**, *27*, 51–56.

(62) Li, Q. B.; Li, F. X.; Jia, L.; Li, Y.; Liu, Y. C.; Yu, J. Y.; Fang, Q.; Cao, A. M. *Biomacromolecules* **2006**, *7*, 2377–2387.

(63) Yu, X. F.; Shi, T. F.; Zhang, G.; An, L. J. *Polymer* **2006**, *47*, 1538–1546.

(64) Miura, Y.; Narumi, A.; Matsuya, S.; Satoh, T.; Duan, Q.; Kaga, H.; Kakuchi, T. *J. Polym. Sci., Part A: Polym. Chem.* **2005**, *43*, 4271–4279.

(65) Miura, Y.; Sakai, Y.; Yamaoka, K. *Macromol. Chem. Phys.* **2005**, *206*, 504–512.

(66) Miura, Y.; Yamaoka, K.; Mannan, M. A. *Polymer* **2006**, *47*, 510–519.

(67) Guo, Y. M.; Pan, C. Y.; Wang, J. J. *J. Polym. Sci., Part A: Polym. Chem.* **2001**, *39*, 2134–2142.

(68) Luan, B.; Zhang, B. Q.; Pan, C. Y. *J. Polym. Sci., Part A: Polym. Chem.* **2006**, *44*, 549–560.

(69) Tunca, U.; Ozyurek, Z.; Erdogan, T.; Hizal, G. *J. Polym. Sci., Part A: Polym. Chem.* **2004**, *42*, 4228–4236.

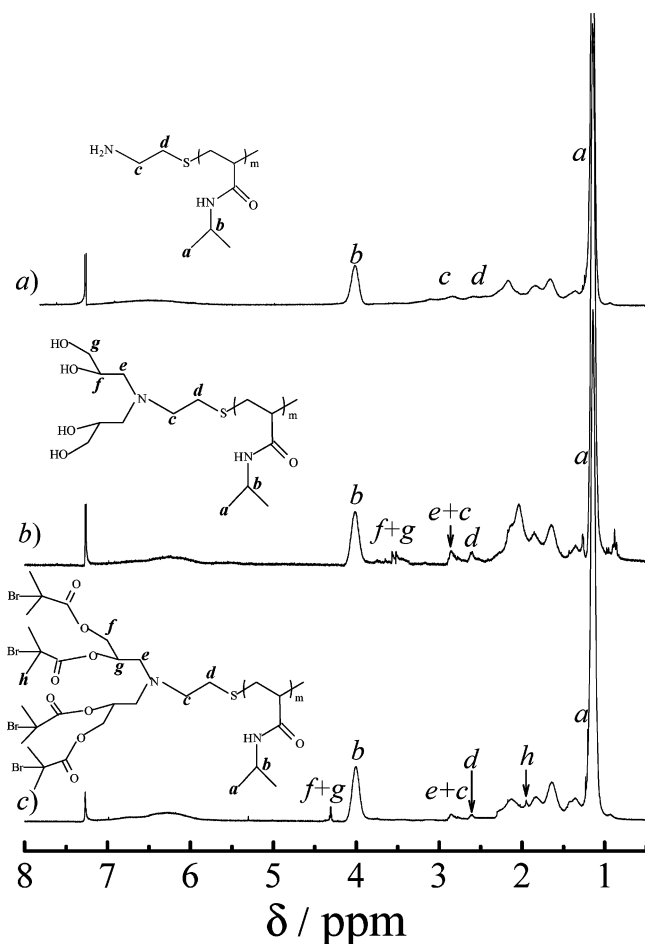


**Figure 1.**  $^1\text{H}$  NMR spectra of (a): PNIPAM- $\text{NH}_2$  (**1a**), (b): PNIPAM-(OH) $_4$ , and (c): PNIPAM-based tetrafunctional ATRP macroinitiator (**1b**) recorded in  $\text{CDCl}_3$ .

protons ( $f + g$ ) (Figure 1c). We can also observe a new signal at  $\delta = 1.9$  ppm ( $h$ ), which was due to the methyl groups of the four terminal bromoisobutryl groups of **1b** (Figure 1c). However, due to its overlapping with the backbone protons, it was impossible to further quantify the degree of esterification based on this signal. A comparison between Figure 1b and 1c told us that the signals at  $\delta = 3.4\text{--}3.7$  ppm completely disappeared, and this strongly suggested the complete esterification of four terminal hydroxyl groups. Compared to **1a**, GPC analysis of **1b** revealed a slight peak shift to higher molecular weight, yielding an  $M_n$  of 7800. The symmetric GPC trace of **1b** told us that the end-group functionalization has no adverse effect on the integrity of the PNIPAM chain.

Tetrafunctional macroinitiator, **1b**, was then used to initiate the ATRP polymerization of DEA monomer. To avoid the deactivation of the copper catalyst through complexation with amide groups of PNIPAM,  $\text{Me}_6\text{TREN}$  was used as the ligand. The monomer conversion was higher than 95% after 12 h. Typical GPC traces of PNIPAM- $\text{NH}_2$  and PNIPAM- $b$ -(PDEA) $_4$  are shown in Figure 2. Both GPC curves were monomodal and quite symmetric, indicating that well-defined nonlinear AB $_4$  block copolymers were successfully obtained. If the resulting nonlinear block copolymer chains contained four, three, or two PDEA branches (which might take place due to the intramolecular irreversible termination reactions or the inefficient initiation during polymerization), the GPC curve should exhibit a tail at the lower molecular weight side. We can at least conclude that the major products are the desired nonlinear miktoarm AB $_4$  block

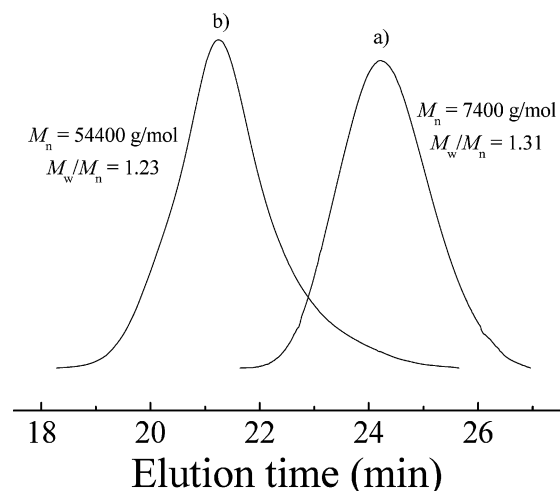


**Figure 2.** THF GPC traces of (a) mono-amino-terminated PNIPAM (**1a**) and (b) PNIPAM $_{65}$ - $b$ -(PDEA $_{63}$ ) $_4$  AB $_4$  miktoarm star copolymer (**1c**).

copolymers (**1c**).<sup>38,68,70</sup> The DP of each PDEA branch was calculated to be 63 from its  $^1\text{H}$  NMR spectrum. Thus the AB $_4$  miktoarm star copolymer, PNIPAM $_{65}$ - $b$ -(PDEA $_{63}$ ) $_4$ , was successfully obtained.

**Synthesis of PNIPAM- $b$ -PDEA Diblock Copolymer through RAFT Polymerization.** The synthetic route for the PNIPAM- $b$ -PDEA diblock copolymer is also shown in Scheme 1. First, a PNIPAM homopolymer (**2a**) with a narrow polydispersity and comparable DP to that of PNIPAM- $\text{NH}_2$  was synthesized via RAFT polymerization. The preparation of PNIPAM- $b$ -PDEA diblock copolymer (**2b**) was achieved using the above PNIPAM as macroRAFT agent. In the process of RAFT polymerization of DEA, a significant low molecular weight shoulder was observed by GPC, probably because a minority of PNIPAM chains lost their dithiobenzoate chain ends. So the product was first extracted with ice-water (at pH 9) to remove any traces of PNIPAM. To further remove the residual DEA monomer, the product was dissolved in acidic water at pH 4 and then dialyzed using semipermeable membrane for 1 day. Thus, residual DEA monomer and PNIPAM homopolymer can be removed. The GPC traces of PNIPAM and purified PNIPAM- $b$ -PDEA are shown in Figure 3. The DP of PNIPAM block is 70, as determined by GPC. The DP of the PDEA block was calculated to be 260, as determined from  $^1\text{H}$  NMR.

**Thermo- and pH-Responsive Micellization of PNIPAM- $b$ -(PDEA) $_4$ .** PNIPAM and PDEA homopolymers exhibit fundamentally different stimuli-responsive solubility. PNIPAM homopolymer dissolves in cold and dilute aqueous solution but becomes insoluble at  $\sim 32^\circ\text{C}$  due to its well-known lower critical solution temperature (LCST) phase behavior.<sup>47</sup> PDEA homopolymer exhibits pH-dependent solubility. It is soluble in acidic solution as a weak cationic polyelectrolyte but phase separates out at around neutral pH.<sup>44,49</sup> For the AB $_4$  miktoarm star copolymer, PNIPAM $_{65}$ - $b$ -(PDEA $_{63}$ ) $_4$ , and linear diblock copolymer, PNIPAM $_{70}$ - $b$ -PDEA $_{260}$ , we can expect that they will exhibit thermoresponsive and pH-responsive ‘schizophrenic’ micellization behavior via a proper combination of solution pH and temperature.

Figure 4 shows the  $^1\text{H}$  NMR spectra recorded for the PNIPAM $_{65}$ - $b$ -(PDEA $_{63}$ ) $_4$  in  $\text{D}_2\text{O}$  at different solution conditions. At  $20^\circ\text{C}$  and pH 4, both PNIPAM and PDEA blocks were

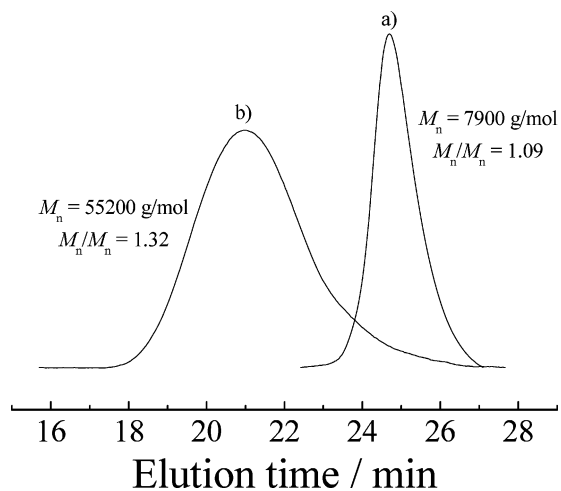


**Figure 3.** THF GPC traces of (a) PNIPAM macroRAFT agent (**2a**) and (b) PNIPAM<sub>70</sub>-*b*-PDEA<sub>260</sub> diblock copolymer (**2b**) after purification.

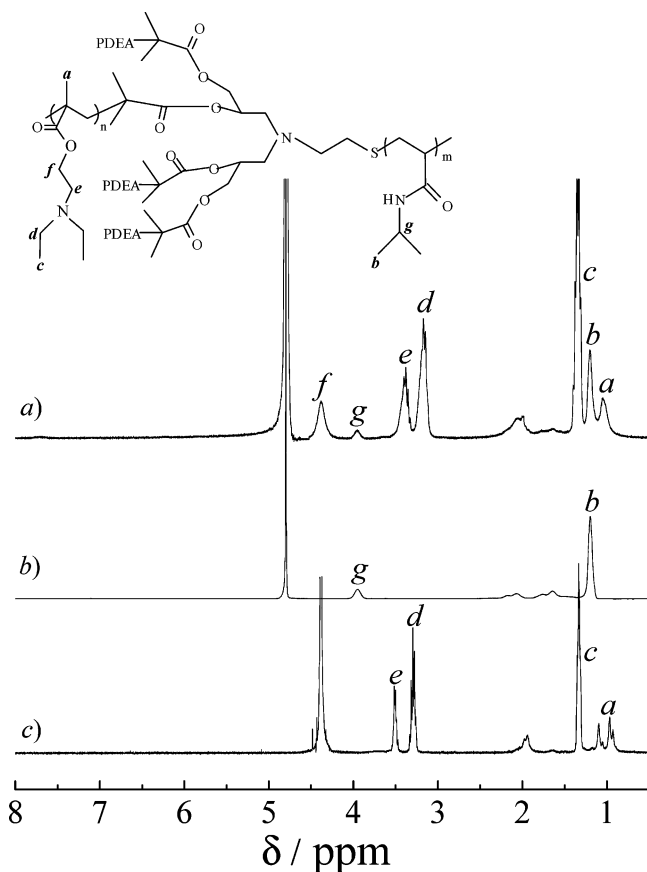


**Figure 4.** <sup>1</sup>H NMR spectra of PNIPAM<sub>65</sub>-*b*-(PDEA<sub>63</sub>)<sub>4</sub> (**1c**) in (a) D<sub>2</sub>O at pH 4 and 20 °C (molecularly dissolved copolymer), (b) D<sub>2</sub>O at pH 10 and 20 °C (PDEA-core micelles), and (c) D<sub>2</sub>O at pH 4 and 40 °C (PNIPAM-core micelles).

hydrophilic, thus the miktoarm star copolymer dissolved molecularly in dilute aqueous solution and <sup>1</sup>H NMR signals due to both blocks were visible (see Figure 2a). Upon addition of a small amount of NaOD into the molecularly dissolved solution at 20 °C, micellization occurred at pH 8 or higher, indicated by the appearance of characteristic bluish tinge (see Figure 4b). Comparing Figure 4a and 4b, it is clear that the signals due to the PDEA block at  $\delta = 1.2, 3.1, 3.5,$  and  $4.4$  ppm completely disappeared. This suggested that PDEA-core micelles were formed,<sup>44,49</sup> with the still-solvated PNIPAM block forming the

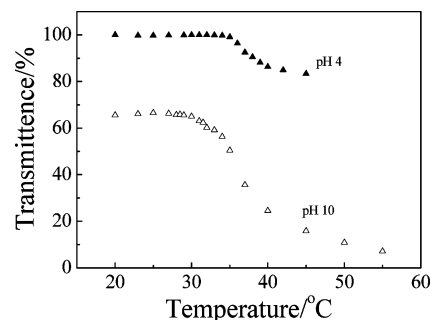


**Figure 5.** Temperature dependence of transmittance of the aqueous solution of PNIPAM<sub>65</sub>-*b*-(PDEA<sub>63</sub>)<sub>4</sub> at pH 4 and pH 10, respectively. The copolymer concentration was 1.0 g/L.

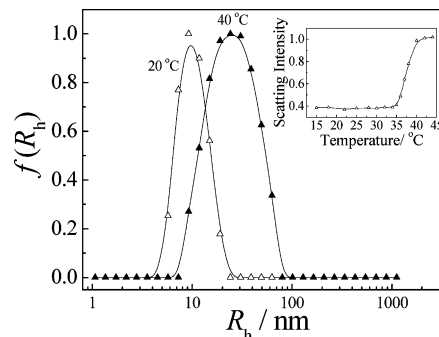


**Figure 6.** Hydrodynamic radius distributions,  $f(R_h)$ , of the aqueous solution of PNIPAM<sub>65</sub>-*b*-(PDEA<sub>63</sub>)<sub>4</sub> at different temperatures (20 and 40 °C) and pH 4; the copolymer concentration was 0.2 g/L. The inset showed the temperature dependence of scattering intensities.

micellar corona. At pH 4 and elevated temperatures, PNIPAM-core micelles were expected to form. Figure 4c shows the <sup>1</sup>H NMR spectrum of PNIPAM<sub>65</sub>-*b*-(PDEA<sub>63</sub>)<sub>4</sub> at pH 4 and 40 °C. It was found that the signals due to PNIPAM block almost disappeared, and the signals due to the PDEA residues were still prominent, suggesting the formation of PNIPAM-core micelles.

Figure 5 shows the variation of transmittance of the aqueous solution of PNIPAM<sub>65</sub>-*b*-(PDEA<sub>63</sub>)<sub>4</sub> as a function of temperature at pH 4 and pH 10, respectively. At pH 4, the transmission decreased only moderately above 35 °C, accompanied with the appearance of bluish tinge, characteristic of micellar solutions. This was in agreement with the formation of PNIPAM-core micelles. The micelles were stabilized by the protonated PDEA block. In marked contrast, at pH 10, heating the initially bluish solution (formation of PDEA-core micelles) above 30 °C led to macroscopic phase separation and hence a turbid solution. At pH 10 and above the LCST, the PNIPAM corona cannot stabilize the hydrophobic PDEA core.<sup>71</sup>

The 'schizophrenic' micellization behavior of PNIPAM<sub>65</sub>-*b*-(PDEA<sub>63</sub>)<sub>4</sub> was further studied by dynamic and static LLS. Figure 6 shows the hydrodynamic radius distributions,  $f(R_h)$ , of PNIPAM<sub>65</sub>-*b*-(PDEA<sub>63</sub>)<sub>4</sub> aqueous solution at different temperatures (20 and 40 °C) and pH 4. The inset showed the temperature dependence of the scattering intensities at pH 4. From the inset, we can see that the scattering light intensities increase considerably when the temperature was above 35 °C, which agreed well with the transmittance results obtained from Figure 5. At 20 °C and pH 4, the miktoarm star copolymer is molecularly dissolved and the solution is clear. The average hydrodynamic radius,  $\langle R_h \rangle$ , is ca. 9 nm. At 40 °C and pH 4, the  $\langle R_h \rangle$  increased to 24 nm, and the increase of scattering intensities at elevated temperatures

(71) Zhang, Y. F.; Luo, S. Z.; Liu, S. Y. *Macromolecules* **2005**, *38*, 9813–9820.

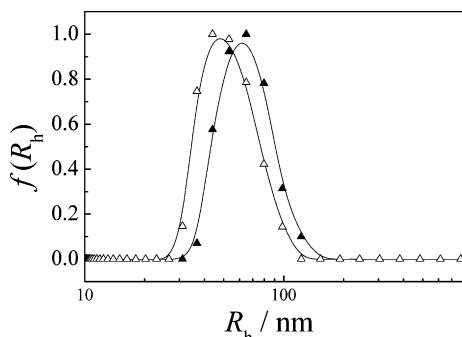


**Figure 7.** Hydrodynamic radius distributions,  $f(R_h)$ , of PDEA-core micelles of PNIPAM<sub>65</sub>-*b*-(PDEA<sub>63</sub>)<sub>4</sub> (Δ) and PNIPAM<sub>70</sub>-*b*-PDEA<sub>260</sub> (▲) at pH 9 and 20 °C; the copolymer concentration was 0.2 g/L.

all confirmed the formation of PNIPAM-core micelles. The polydispersity indexes of the size distributions ( $\mu_2/\Gamma^2$ ) of the aqueous solution of PNIPAM<sub>65</sub>-*b*-(PDEA<sub>63</sub>)<sub>4</sub> at 20 and 40 °C (at pH 4) were 0.14 and 0.18, respectively. Apparently, PNIPAM<sub>70</sub>-*b*-PDEA<sub>260</sub> exhibited similar thermoresponsive micellization behavior, and the details have not been further checked in the present study.

At pH 10 and room temperature, both the miktoarm AB<sub>4</sub> and linear AB copolymers formed PDEA-core micelles. Figure 7 shows the hydrodynamic radius distributions,  $f(R_h)$ , of PNIPAM<sub>65</sub>-*b*-(PDEA<sub>63</sub>)<sub>4</sub> and PNIPAM<sub>70</sub>-*b*-PDEA<sub>260</sub> micelles at pH 10 and a copolymer concentration of 0.2 g/L. Clearly, the PDEA-core micelles of PNIPAM<sub>65</sub>-*b*-(PDEA<sub>63</sub>)<sub>4</sub> were smaller than that of PNIPAM<sub>70</sub>-*b*-PDEA<sub>260</sub>, and the  $\langle R_h \rangle$  of both micelles were 41 and 64 nm, respectively. Both micelles were relatively narrow-disperse with  $\mu_2/\Gamma^2$  of  $\sim 0.1$ . Based on the above discussion, a schematic illustration for the ‘schizophrenic’ micellization of PNIPAM-*b*-(PDEA)<sub>4</sub> is summarized in Figure 8.

The two copolymer micelles were further characterized by static LLS, and the results are summarized in Table 1. The apparent molar masses of the PDEA-core micelles of PNIPAM<sub>65</sub>-*b*-(PDEA<sub>63</sub>)<sub>4</sub> and PNIPAM<sub>70</sub>-*b*-PDEA<sub>260</sub> were  $7.6 \times 10^6$  and  $1.2 \times 10^7$  g/mol, respectively. The aggregation numbers of both micelles were 140 and 210, respectively. The PDEA-core micelles of PNIPAM<sub>65</sub>-*b*-(PDEA<sub>63</sub>)<sub>4</sub> have a larger density (0.044 g/cm<sup>3</sup>) than that of PNIPAM<sub>70</sub>-*b*-PDEA<sub>260</sub> (0.018 g/cm<sup>3</sup>). This was in agreement with the results obtained by Pispas et al.<sup>28</sup> They reported that AB<sub>2</sub> Y-shaped block copolymers formed micelles with smaller size and lower aggregation number compared to that of the AB linear diblock copolymer with similar block composition and molecular weight. On the basis of the simple scaling theory developed by Pispas et al.,<sup>28</sup> the branching of the PDEA block in the case of PNIPAM<sub>70</sub>-*b*-PDEA<sub>260</sub> increased the elastic energy of the stretching of the insoluble PDEA block inside the micellar core. Thus, the aggregation number needed to be decreased to compensate the fixed gain in aggregation energy. If the PDEA-core micelles of PNIPAM<sub>65</sub>-*b*-(PDEA<sub>63</sub>)<sub>4</sub> and PNIPAM<sub>70</sub>-*b*-PDEA<sub>260</sub> copolymers had the same aggregation number, it was reasonable to expect that the former would form smaller micelles with larger densities due to the possibility of more compact packing of the branched PDEA arms. In our case, the aggregation number of PDEA-core micelles of PNIPAM<sub>65</sub>-*b*-(PDEA<sub>63</sub>)<sub>4</sub> was lower than that of PNIPAM<sub>70</sub>-*b*-PDEA<sub>260</sub>, so it was quite understandable that the former formed smaller micelles.

**pH-Induced Micellization Kinetics of AB<sub>4</sub> Miktoarm Star and AB Block Copolymers.** We then further studied the pH-induced micellization kinetics of PDEA-core micelles of PNIPAM<sub>65</sub>-*b*-(PDEA<sub>63</sub>)<sub>4</sub> and PNIPAM<sub>70</sub>-*b*-PDEA<sub>260</sub> upon a pH jump from acidic to alkaline conditions. The pH jump was realized

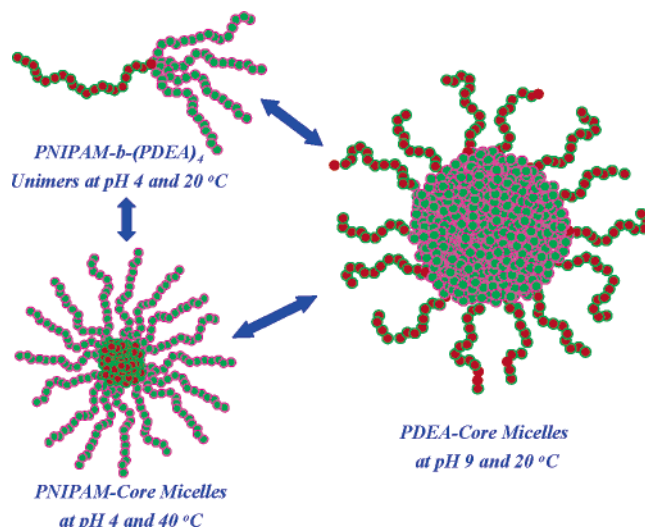


**Figure 8.** A schematic illustration of the ‘schizophrenic’ micellization behavior of PNIPAM-*b*-(PDEA)<sub>4</sub> miktoarm star copolymer. Unimers, PDEA-core micelles, and PNIPAM-core micelles were formed at different solution conditions.

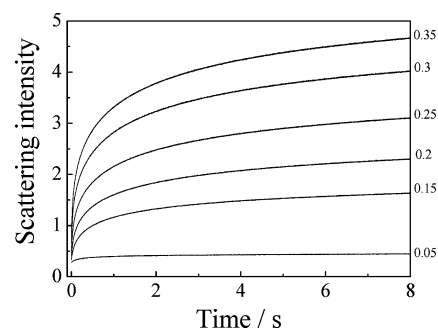


**Figure 9.** Time dependence of the scattering light intensities of aqueous solutions of PNIPAM<sub>65</sub>-*b*-(PDEA<sub>63</sub>)<sub>4</sub> upon a pH jump from 4 to 10 at 20 °C. From bottom to top, the final copolymer concentration ranged from 0.05 to 0.35 g/L.

by stopped-flow mixing the polymer solution with aqueous NaOH solution. Typical dynamic traces of the micellization process for PNIPAM<sub>65</sub>-*b*-(PDEA<sub>63</sub>)<sub>4</sub> upon a pH jump from 4 to 10 at different final polymer concentrations are shown in Figure 9. If the final copolymer concentration is lower than 0.05 g/L, we did not observe any relaxation processes, and the dynamic curve remained a straight line. At a final polymer concentration of 0.05 g/L, we can discern a moderate increase of scattering intensities. Based on our previous studies of the pH-induced micellization kinetics of PGMA-*b*-PDMA-*b*-PDEA,<sup>45</sup> the cmc of the PDEA-core micelles of PNIPAM<sub>65</sub>-*b*-(PDEA<sub>63</sub>)<sub>4</sub> was determined to be  $\sim 0.05$  g/L.

When the final copolymer concentration was larger than 0.05 g/L, relaxation process with positive amplitudes was always observed (Figure 9). The time dependence of the scattering light intensity  $I_t$  can be converted to a normalized function, namely,  $(I_\infty - I_t)/I_\infty$  vs  $t$ , where  $I_\infty$  is the value of  $I_t$  at an infinitely long time. A single-exponential function cannot fit the relaxation curve very well (Figure 10, top), especially for the first 0.5 s, which is the most interesting to us because kinetics are the most accurate at their initial stages. Empirically, we found that such a function could be well fitted by a double-exponential function (Figure 10, bottom):

$$(I_\infty - I_t)/I_\infty = c_1 e^{-t/\tau_1} + c_2 e^{-t/\tau_2} \quad (2)$$

where  $c_1$  and  $c_2$  are the normalized amplitudes ( $c_2 = 1 - c_1$ ),

**Table 1.** LLS Characterization Results of PDEA-Core Micelles of PNIPAM<sub>65</sub>-*b*-(PDEA<sub>63</sub>)<sub>4</sub> and PNIPAM<sub>70</sub>-*b*-PDEA<sub>260</sub> at pH 9 and 20 °C<sup>a</sup>

samples	$\langle R_g \rangle$ (nm)	$\langle R_h \rangle$ (nm)	$\langle R_g \rangle / \langle R_h \rangle$	$M_{w, app}$	$N_{agg}$
PNIPAM <sub>65</sub> - <i>b</i> -(PDEA <sub>63</sub> ) <sub>4</sub>	23	41	0.56	$7.6 \times 10^6$	140
PNIPAM <sub>70</sub> - <i>b</i> -PDEA <sub>260</sub>	40	64	0.63	$1.2 \times 10^7$	210

<sup>a</sup> The copolymer concentration is 0.2 g/L.

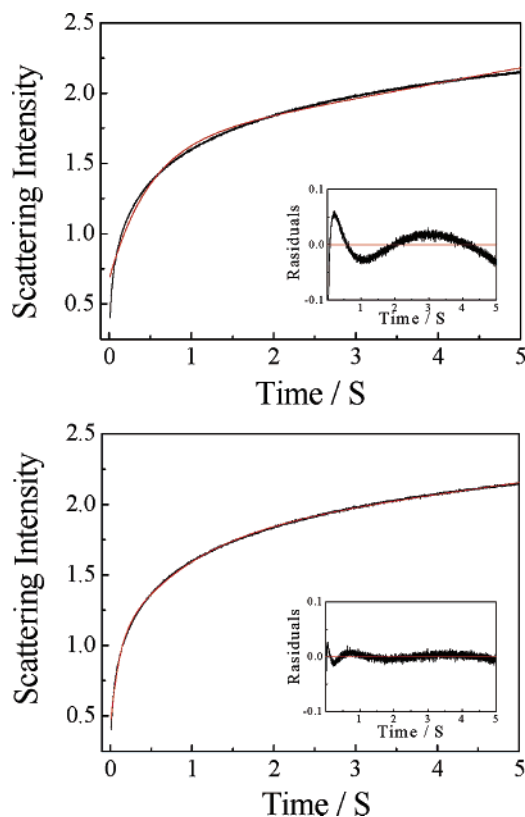


**Figure 10.** Typical time dependence of the scattering light intensities recorded during micelle formation from PNIPAM<sub>65</sub>-*b*-(PDEA<sub>63</sub>)<sub>4</sub> induced by a pH jump from 4 to 10. The top and bottom figures were fitted by single and double exponential functions, respectively. The copolymer concentration was 0.2 g/L and the temperature was 20 °C.

$\tau_1$  and  $\tau_2$  are the characteristic relaxation times of two processes,  $\tau_1 < \tau_2$ . Both  $\tau_1$  and  $\tau_2$  have positive amplitudes. The overall relaxation time for the micellization process,  $\tau_f$ , can be calculated as

$$\tau_f = c_1\tau_1 + c_2\tau_2 \quad (3)$$

All the dynamic curves in Figure 9 can be well fitted with a double-exponential function.  $\tau_1$ ,  $\tau_2$ , and the calculated  $\tau_f$  based on eq 3 are shown in Figure 11.  $\tau_1$  was in the range 0.05–0.15 s and decreases with copolymer concentration.  $\tau_2$  was  $\sim 0.8$ –0.9, which was essentially independent of polymer concentrations in the range studied.  $\tau_f$  for the overall micelle formation process was in the range 0.4–0.6 s, which decreased with polymer concentrations.

In the same concentration range, the pH-induced micelle formation kinetics of PNIPAM<sub>70</sub>-*b*-PDEA<sub>260</sub> was also studied. The polymer concentration dependence of  $\tau_1$ ,  $\tau_2$ , and  $\tau_f$  for the micellization processes are shown in Figure 12.  $\tau_1$ ,  $\tau_2$ , and  $\tau_f$  were in the range 0.12–0.2 s, 1.0–1.3 s, and 0.8–1 s, respectively. All of the three relaxation times decreased with polymer concentrations. The kinetics of the micellization of PNIPAM<sub>70</sub>-*b*-PDEA<sub>260</sub> was systematically slower than that of PNIPAM<sub>65</sub>-*b*-(PDEA<sub>63</sub>)<sub>4</sub>. We thus found that the pH-induced micellization

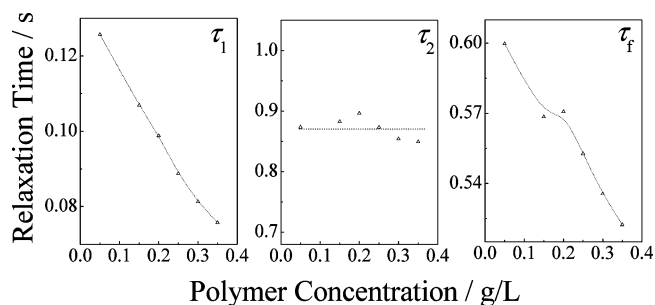


**Figure 11.** Double-exponential fitting results obtained from the micelle formation kinetics at various final PNIPAM<sub>65</sub>-*b*-(PDEA<sub>63</sub>)<sub>4</sub> concentrations. The experimental conditions are the same to Figure 9.

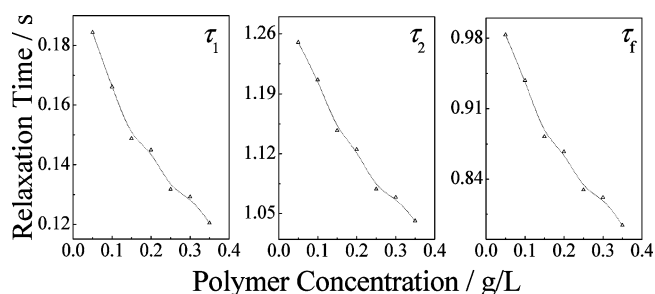


**Figure 12.** Double-exponential fitting results obtained from the micelle formation kinetic traces upon a pH jump from 4 to 10 for PNIPAM<sub>70</sub>-*b*-PDEA<sub>260</sub> diblock copolymer at different final polymer concentrations. The temperature was fixed at 20 °C.

kinetics of PNIPAM<sub>65</sub>-*b*-(PDEA<sub>63</sub>)<sub>4</sub> and PNIPAM<sub>70</sub>-*b*-PDEA<sub>260</sub> exhibit some fundamental differences.

For the unimer-to-micelle transition of block copolymers, Mattice et al.<sup>72</sup> performed computer simulations that suggested the presence of two processes with different time scales: the volume fraction of free chains reaches its equilibrium value very quickly in the fast step, followed by a slower step toward the equilibrium state. Dormidontova and co-workers<sup>39,73,74</sup> further proposed a micelle fusion/fission–unimer expulsion/entry joint mechanism for the formation of block copolymer micelles. Rapid micelle fusion/fission dominated over unimer entry/expulsion initially (fast process), while the latter process dominated on longer time scales (the slow process). In our previous investigation of the pH-induced micellization of PGMA-*b*-PDMA-*b*-PDEA triblock copolymer, we have interpreted the kinetic data in the frame of above theoretical considerations.<sup>45</sup>

For the pH-induced micellization of PNIPAM<sub>65</sub>-*b*-(PDEA<sub>63</sub>)<sub>4</sub> and PNIPAM<sub>70</sub>-*b*-PDEA<sub>260</sub> upon a pH jump from 4 to 10, the relaxation time of the fast process ( $\tau_1$ ) for both copolymers decreased with increasing copolymer concentration. The fast process was known to be associated with the quick association of unimers into large amounts of small micelles and the formation of quasi-equilibrium micelles. Thus, the growth of small micelles

(72) Wang, Y. M.; Mattice, W. L.; Napper, D. H. *Langmuir* **1993**, *9*, 66–70.

(73) Esselink, F. J.; Dormidontova, E.; Hadziioannou, G. *Macromolecules* **1998**, *31*, 2925–2932.

(74) Esselink, F. J.; Dormidontova, E. E.; Hadziioannou, G. *Macromolecules* **1998**, *31*, 4873–4878.

for PNIPAM<sub>65</sub>-*b*-(PDEA<sub>63</sub>)<sub>4</sub> and PNIPAM<sub>70</sub>-*b*-PDEA<sub>260</sub> and their growth into quasiequilibrium micelles proceeded mainly via the fusion/fission mechanism.  $\tau_1$  of PNIPAM<sub>65</sub>-*b*-(PDEA<sub>63</sub>)<sub>4</sub> was systematically smaller than that of PNIPAM<sub>70</sub>-*b*-PDEA<sub>260</sub>. The fast process was associated partially with the diffusion rate of unimer chains. At comparable composition and molecular weight, the hydrodynamic volume of the branched AB<sub>4</sub> copolymer will be smaller than that of the AB diblock copolymer; thus, the translational diffusion coefficient,  $D$ , of the former will be larger than that of the latter. Thus we can reasonably explain the obtained smaller  $\tau_1$  for the AB<sub>4</sub> miktoarm star copolymer compared to that of the linear AB diblock copolymer.

The slow process ( $\tau_2$ ) was associated with micelle formation/breakup, leading to micelles with larger aggregation numbers and lower number density of micelles. Two mechanisms, unimer entry/expulsion and micelle fusion/fission, may take effect in this slow process. For block copolymers, the characteristic relaxation time for a copolymer chain to escape from the micelles has been theoretically discussed by Halperin and Alexander<sup>40</sup> on the basis of scaling analysis within the context of Aniansson and Wall (A-W) theory<sup>75</sup> for small molecule surfactants. Their main conclusion was that the entry/expulsion of individual chains (unimer exchange) is the only mechanism for block copolymer micelle evolution. Extensive temperature jump (typically  $\Delta T = 1-2$  °C) experiments conducted on E<sub>n</sub>P<sub>m</sub>E<sub>n</sub> triblock copolymers (where E<sub>n</sub> = poly(ethylene oxide) and P<sub>m</sub> = poly(propylene oxide)) using light scattering detection have partially verified the proposed micellization dynamics.<sup>76-78</sup> However, there existed evidence that micelle fission/fusion may also play an important role,<sup>79-82</sup> which is contrary to Halperin and Alexander's predictions.<sup>40</sup>

From Figure 11 we can tell that  $\tau_2$  of PNIPAM<sub>65</sub>-*b*-(PDEA<sub>63</sub>)<sub>4</sub> was independent of copolymer concentration, which suggested the micelle formation/breakup in the slow process proceeds via the unimer entry/expulsion mechanism.<sup>45</sup> Otherwise, we should observe the decrease of  $\tau_2$  with polymer concentration because larger polymer concentrations will lead to faster micelle fusion. This is similar to our previous studies of the micellization kinetics of PGMA-*b*-PDMA-*b*-PDEA.<sup>45</sup> From Figure 12, we know that  $\tau_2$  of PNIPAM<sub>70</sub>-*b*-PDEA<sub>260</sub> decreases with increasing copolymer concentration, suggesting that the slow process for the linear PNIPAM<sub>70</sub>-*b*-PDEA<sub>260</sub> proceeds via the fusion/fission mechanism.

The fundamental differences in the mechanisms of the slow process can be explained in terms of the extent of stretching of coronal PNIPAM chains. From the structural parameters of the two types of micelles listed in Table 1, we can calculate that the density of PDEA-core micelles of the AB<sub>4</sub> miktoarm star

copolymer is about twice as that of the AB linear diblock copolymer. This will lead to a smaller surface area per PNIPAM chain at the core-shell interface for the AB<sub>4</sub> case, i.e., the PNIPAM coronal chains will be more stretched. Thus we can reasonably speculate that for PNIPAM<sub>65</sub>-*b*-(PDEA<sub>63</sub>)<sub>4</sub>, the fusion/fission of quasiequilibrium micelles in the second process will be less favorable compared to that of PNIPAM<sub>70</sub>-*b*-PDEA<sub>260</sub>.

The calculated  $\tau_f$  based on eq 3 for the overall micellization process of PNIPAM<sub>65</sub>-*b*-(PDEA<sub>63</sub>)<sub>4</sub> was smaller than that of PNIPAM<sub>70</sub>-*b*-PDEA<sub>260</sub>, possibly due to that the former formed micelles with much lower aggregation numbers. The larger translational diffusion coefficient of PNIPAM<sub>65</sub>-*b*-(PDEA<sub>63</sub>)<sub>4</sub> may also contribute to the observed differences.

## Conclusions

Well-defined double hydrophilic miktoarm AB<sub>4</sub> star copolymer, PNIPAM-*b*-(PDEA)<sub>4</sub>, was synthesized by polymerizing 2-(diethylamino)ethyl methacrylate (DEA) via atom transfer radical polymerization (ATRP) in 2-propanol at 45 °C using a tetrafunctional initiator, where PNIPAM was poly(*N*-isopropylacrylamide) and PDEA was poly(2-(diethylamino)ethyl methacrylate). To study the chain architectural effects on the micellar properties and kinetics, PNIPAM-*b*-PDEA linear diblock copolymer with comparable molecular weight and composition to that of PNIPAM-*b*-(PDEA)<sub>4</sub> was also prepared. The pH- and thermoresponsive 'schizophrenic' micellization behavior of the obtained PNIPAM<sub>65</sub>-*b*-(PDEA<sub>63</sub>)<sub>4</sub> miktoarm star and PNIPAM<sub>70</sub>-*b*-PDEA<sub>260</sub> linear diblock copolymers were investigated by a combination of <sup>1</sup>H NMR and laser light scattering (LLS). In acidic solution and elevated temperatures, PNIPAM-core micelles were formed. At slightly alkaline condition and room temperature, structurally inverted PDEA-core micelles were formed. The size of the PDEA-core micelles of PNIPAM<sub>65</sub>-*b*-(PDEA<sub>63</sub>)<sub>4</sub> is much smaller than that of PNIPAM<sub>70</sub>-*b*-PDEA<sub>260</sub>. Furthermore, the pH-induced micellization kinetics of the AB<sub>4</sub> miktoarm star and AB block copolymers were investigated by the stopped-flow light scattering technique upon a pH jump from 4 to 10. Typical kinetic traces for the micellization of both copolymers can be well fitted with double exponential functions, yielding a fast ( $\tau_1$ ) and a slow ( $\tau_2$ ) relaxation processes.  $\tau_1$  for both copolymers decreased with increasing polymer concentration.  $\tau_2$  was independent of polymer concentration for PNIPAM<sub>65</sub>-*b*-(PDEA<sub>63</sub>)<sub>4</sub>, suggesting that the micelle formation/breakup in the slow process proceeded via the unimer entry/expulsion mechanism.  $\tau_2$  decreased with increasing polymer concentration for PNIPAM<sub>70</sub>-*b*-PDEA<sub>260</sub>, which suggested that the slow process for the linear PNIPAM<sub>70</sub>-*b*-PDEA<sub>260</sub> proceeds via the fusion/fission mechanism. An explanation for the fundamental differences in the micellization mechanisms was tentatively proposed.

**Acknowledgment.** This work was financially supported by an Outstanding Youth Fund (50425310) and research grants (20534020, 20674079) from the National Natural Scientific Foundation of China (NNSFC), the "Bai Ren" Project of the Chinese Academy of Sciences, and the Program for Changjiang Scholars and Innovative Research Team in University (PCSIRT).

LA062719B

(75) Aniansson, E. A. G.; Wall, S. N.; Almgren, M.; Hoffmann, H.; Kielmann, I.; Ulbricht, W.; Zana, R.; Lang, J.; Tondre, C. *J. Phys. Chem.* **1976**, *80*, 905-922.

(76) Goldmints, I.; Holzwarth, J. F.; Smith, K. A.; Hatton, T. A. *Langmuir* **1997**, *13*, 6130-6134.

(77) Michels, B.; Waton, G.; Zana, R. *Langmuir* **1997**, *13*, 3111-3118.

(78) Goldmints, I.; vonGottberg, F. K.; Smith, K. A.; Hatton, T. A. *Langmuir* **1997**, *13*, 3659-3664.

(79) Kositzka, M. J.; Bohne, C.; Alexandridis, P.; Hatton, T. A.; Holzwarth, J. F. *Macromolecules* **1999**, *32*, 5539-5551.

(80) Kositzka, M. J.; Bohne, C.; Alexandridis, P.; Hatton, T. A.; Holzwarth, J. F. *Langmuir* **1999**, *15*, 322-325.

(81) Waton, G.; Michels, B.; Zana, R. *Macromolecules* **2001**, *34*, 907-910.

(82) Kositzka, M. J.; Bohne, C.; Hatton, T. A.; Holzwarth, J. F. *Trends Colloid Interface Sci.* **1999**, *112*, 146-151.